AFRL-PR-WP-TP-2007-241

INFLUENCE OF AN ADDITIONAL BALLAST VOLUME ON A PULSED ICP DISCHARGE (POSTPRINT)

E.A. Bogdanov, C.A. DeJoseph, Jr., V.I. Demidov, A.A. Kudryavtsev, and K. Yu Serditov

Electrical Technology & Plasma Physics Branch
Power Division

AUGUST 2007

AIR FORCE RESEARCH LABORATORY
PROPULSION DIRECTORATE
WRIGHT-PATTERSON AIR FORCE BASE, OH 45433-7251
AIR FORCE MATERIEL COMMAND
UNITED STATES AIR FORCE

REPORT DOCUMENTATION PAGE

Form Approved
OMB No. 0704-0188

1. REPORT DATE *(DD-MM-YY)*	2. REPORT TYPE	3. DATES COVERED *(From - To)*
August 2007	Journal Article Postprint	01 January 2007 – 01 August 2007

4. TITLE AND SUBTITLE
INFLUENCE OF AN ADDITIONAL BALLAST VOLUME ON A PULSED ICP DISCHARGE (POSTPRINT)

5a. CONTRACT NUMBER
In-house

5b. GRANT NUMBER

5c. PROGRAM ELEMENT NUMBER
61102F

6. AUTHOR(S)
E.A. Bogdanov, A.A. Kudryavtsev, and K. Yu Serditov (St. Petersburg State University)
C.A. DeJoseph, Jr. (AFRL/PRPE)
V.I. Demidov (West Virginia University)

5d. PROJECT NUMBER
2301

5e. TASK NUMBER
DW

5f. WORK UNIT NUMBER
2301DW23

7. PERFORMING ORGANIZATION NAME(S) AND ADDRESS(ES)

St. Petersburg State University
St. Petersburg 198904, Russia

West Virginia University
Department of Physics
Morgantown, WV 26506

Electrical Technology & Plasma Physics Branch (AFRL/PRPE)
Power Division
Air Force Research Laboratory, Propulsion Directorate
Wright-Patterson Air Force Base, OH 45433-7251
Air Force Materiel Command, United States Air Force

8. PERFORMING ORGANIZATION REPORT NUMBER
AFRL-PR-WP-TP-2007-241

9. SPONSORING/MONITORING AGENCY NAME(S) AND ADDRESS(ES)
Air Force Research Laboratory
Propulsion Directorate
Wright-Patterson Air Force Base, OH 45433-7251
Air Force Materiel Command
United States Air Force

10. SPONSORING/MONITORING AGENCY ACRONYM(S)
AFRL/PRPE

11. SPONSORING/MONITORING AGENCY REPORT NUMBER(S)
AFRL-PR-WP-TP-2007-241

12. DISTRIBUTION/AVAILABILITY STATEMENT
Approved for public release; distribution unlimited.

13. SUPPLEMENTARY NOTES
Journal article published in the *Plasma Sources Science and Technology Journal*, Vol. 16, 2007. © 2007 IOP Publishing Ltd. The U.S. Government is joint author of this work and has the right to use, modify, reproduce, release, perform, display, or disclose the work. PAO Case Number: AFRL/WS 07-2007, 28 Aug 2007.

14. ABSTRACT
A spatial and temporal numerical simulation has been carried out of a pulsed (100% modulated), rf inductively coupled plasma discharge in argon, connected to an additional (ballast) diffusion chamber of much larger volume. It is demonstrated that during the active phase, the presence of the large ballast volume has a small impact on the parameters of the plasma in the smaller discharge chamber. In this case the plasma parameters in the discharge chamber can be estimated separately from the diffusion chamber by a standard method using the characteristic ambipolar diffusion time (for example, using a global model). However, during the afterglow phase, the situation is changed significantly. In the afterglow, the densities of charged particles in the discharge chamber become lower than in the large ballast chamber due to more rapid diffusion loss. As a result, the reverse of the active phase situation occurs, namely, the plasma does not flow from the small to the large chamber, but in the opposite direction, from diffusive to discharge volume, and both the plasma density gradient and the self-consistent ambipolar electric field in the small chamber change directions.

15. SUBJECT TERMS
Pulsed radio frequency discharge, plasma afterglow, detachment

16. SECURITY CLASSIFICATION OF:			17. LIMITATION OF ABSTRACT:	18. NUMBER OF PAGES	19a. NAME OF RESPONSIBLE PERSON (Monitor)
a. REPORT	b. ABSTRACT	c. THIS PAGE			C.A. DeJoseph, Jr.
Unclassified	Unclassified	Unclassified	SAR	12	19b. TELEPHONE NUMBER *(Include Area Code)* N/A

Standard Form 298 (Rev. 8-98)
Prescribed by ANSI Std. Z39-18

Plasma Sources Sci. Technol. **16** (2007) 1–6 UNCORRECTED PROOF

Influence of an additional ballast volume on a pulsed ICP discharge

E A Bogdanov[1], C A DeJoseph Jr[2], V I Demidov[3], A A Kudryavtsev[1] and K Yu Serditov[1]

[1] St Petersburg State University, St Petersburg 198904, Russia
[2] Air Force Research Laboratory, Wright-Patterson AFB, OH 45433, USA
[3] Department of Physics, West Virginia University, Morgantown, WV 26506, USA

E-mail: charles.dejoseph@wpafb.af.mil

Received 30 March 2007, in final form 15 June 2007
Published
Online at stacks.iop.org/PSST/16

Abstract

A spatial and temporal numerical simulation has been carried out of a pulsed (100% modulated), rf inductively coupled plasma discharge in argon, connected to an additional (ballast) diffusion chamber of much larger volume. It is demonstrated that during the active phase, the presence of the large ballast volume has a small impact on the parameters of the plasma in the smaller discharge chamber. In this case the plasma parameters in the discharge chamber can be estimated separately from the diffusion chamber by a standard method using the characteristic ambipolar diffusion time (for example, using a global model). However, during the afterglow phase, the situation is changed significantly. In the afterglow, the densities of charged particles in the discharge chamber become lower than in the large ballast chamber due to more rapid diffusion loss. As a result, the reverse of the active phase situation occurs, namely, the plasma does not flow from the small to the large chamber, but in the opposite direction, from diffusive to discharge volume, and both the plasma density gradient and the self-consistent ambipolar electric field in the small chamber change directions. This phenomenon leads to new effects in the discharge volume, in particular a decreasing rate of decay of densities of charged particles and electron temperature. Thus, in the afterglow the presence of a large additional ballast volume has a significant impact on the plasma transport. In this case, a simple treatment of the plasma in the discharge chamber in the framework of a spatially averaged model (for example, the global model) is inadequate.

AQ1 (Some figures in this article are in colour only in the electronic version)

1. Introduction

Utilization of a pulsed or modulated discharge is a possible approach for optimizing and improving the various plasmo-chemical reactors and devices for plasma processing, etching, production of nanotubes, etc. By varying the duration of the active phase, repetition frequency, deposition power and other external parameters it is possible to gain increased control of various plasma characteristics and therefore achieve improvement in the operation of these devices [1, 2].

For describing and optimizing these systems both large-scale computational codes (see, for example, [3–12]) and simple analytical models are widely used. These allow quick estimation of plasma parameters, prediction of the discharge behavior and developing scaling laws over a range of conditions. In the last case, the most common approach is based on the utilization of spatially averaged models (see, for example, [33]) when the diffusion of particles of type j is estimated through their effective diffusion time $\tau_j = \Lambda^2/D_j$, where Λ is the diffusion length of the discharge volume,

JNL: PSST PIPS: 247569 TYPE: PAP TS: NEWGEN DATE: 6/8/2007 EDITOR: MK

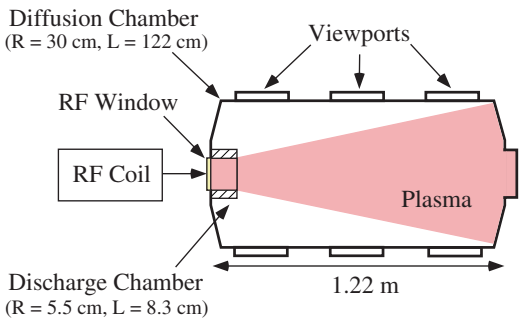

Figure 1. Schematic diagram of the experimental setup.

which for a cylinder is $R/2.4$, where R is the radius of the cylinder and D_j is the diffusion coefficient of the particle. For more complicated geometries, the reactor's effective diffusion length, in the simplest approximation, can be estimated as a ratio of the volume to the surface area, $\Lambda \approx V/S$. For steady-state as well as for pulse discharges many calculations using this approach have been published, and following a series of papers, [14–17] is frequently referred to as the 'Global model'.

Application of the Global model for pulsed discharges may be somewhat more difficult than steady-state situations and it may be important to take into account design features of the reactor which, at first glance, may not seem necessary. An example of this situation is described and presented in this paper. Many plasma processing systems use a relatively small discharge volume connected to a much larger diffusion, or ballast, chamber. In non-stationary discharges the presence of the two significantly different discharge and ballast volumes may, under certain circumstances, lead to unexpected results. Specifically, the ballast volume, which accumulates energy and particles from the discharge chamber during the active phase, can return these during the afterglow. The application of simple average models, which do not take this into account, can lead to significant errors.

Thus, the aim of this paper is to study the plasma characteristic in a pulsed rf inductively coupled plasma (ICP) discharge, initiated in a small chamber, which is connected to a diffusion chamber of a much greater volume.

2. Experimental setup for simulations

The simulations in this work were performed for the system used in our previous work [18–20], where details of the experiment can be found. A simplified schematic diagram of the setup is shown in figure 1. The system volume is divided into two chambers. The rf ICP discharge is created in a small chamber (discharge chamber in figure 1) with a length of 8.3 cm and a radius of 5.5 cm. The plasma can diffuse into the large volume (diffusion chamber), with a length of 122 cm and a radius of 30 cm. Working gas is argon at pressures between 5 and 30 mTorr. Power deposited in the discharge varies, typically, over the range from 5 to 300 W with an active phase of the discharge from 100 to 300 μs and an afterglow phase from 1 to 3 ms. Current and voltage probes are used to measure rf power into the coil.

It should be noted that both probe (see, for example [21]) as well as optical (see, for example, [22]) diagnostics are well developed for rf ICP discharges. In particular, emission spectroscopy allows spatial and temporal measurement of excited states of atoms [23, 24]. However, for ICP discharges of the specific geometry, including additional ballast volume, shown in figure 1, there are no detailed results from either experiments or simulations. This paper presents results of simulations only. Experimental confirmation of the effects outlined here will be provided in a future publication.

3. Simulation model

A full-scale 2D simulation of the above plasma reactor in argon has been performed using the methodology previously developed [25]. The main input parameters for the simulations are as follows: geometry of the discharging volume, pressure and composition of gas and rf power deposited in the plasma (or current in the coils). Early simulations showed that the frequently used three level scheme, including only the ground state, one excited state, namely, the metastable level (see, for example, [7]), and the ion ground state resulted in large discrepancies when compared with measurements of afterglow parameters. By including a resonant level, energetically close to the metastable level, acceptable accuracy in the simulation was achieved. This resonant level mixes effectively with the metastable level, which is especially important in describing the afterglow. Therefore, for the simulations reported here, this four level model was used. The balance between metastable and resonance atoms strongly depends on both direct excitation from the ground state, but also on cascade contributions from higher excited states. Cascade contributions were taken into account using the approach of Pitchford *et al* [27], i.e. the total flux from higher levels is partitioned into metastable and resonant levels in a fixed ratio which can be set in the simulation (in the simplest case 1 : 1). Rate constants for processes involving electrons and their transport coefficients and in equations for densities (n_e) and average electron energy (temperature T_e), as well as densities of metastable (n_m) and resonance (n_r) levels, were found using calculated electron energy distributions (EED). The EED has been found from the Boltzman transport equation, taking into account electron heating by the electric field and energy exchange through elastic, electron–electron and inelastic collisions. The set of physicochemical reactions used in the simulations are shown in table 1.

The set of the ion balance equations, written in the drift–diffusion approximation, and the EED were solved numerically using the CFDRC software [4]. This code is capable of handling a variety of plasma systems, one of which is the pulsed ICP plasma. A detailed self-consistent model of the discharge plasma, numerical iteration scheme and technique for solving the set of equations are described in detail in [28], and examples of how this scheme is used to solve different plasma problems can be found in [25, 26, 29, 31, 32].

4. Simulation results

Typical results of the 2D simulations of the spatial distribution of electron density at the end of the active discharge phase and 500 μs in the afterglow are presented in figures 2 and 3. As might be expected, the peak electron density during the active phase occurs in the discharge (small) chamber not too

Table 1. Set of plasma reactions used in the model.

#	Fraction	ϵ (eV)	Constant	Comment
1	$e + Ar \rightarrow e + Ar$	—	Cross section [33]	Momentum transfer
2	$e + Ar \rightarrow e + Ar_m^*$	11.5	Effective cross section compiled from [33, 34]	Metastable state excitation (11.55 eV)
3	$e + Ar \rightarrow e + Ar_r^*$	11.67	Effective cross section compiled from [33, 34]	Resonant state excitation (11.67 eV)
4	$e + Ar \rightarrow 2e + Ar^+$	15.9	Cross section [33]	Direct inonization
5	$e + Ar_m^* \rightarrow 2e + Ar^+$	4.35	Cross section [36]	Stepwise ionization
6	$e + Ar_m^* \leftrightarrow 2e + Ar_r^*$	0.07	$k_p = 1 \times 10^{13}\ m^3\ s^{-1}$ [35]	Mixing from metastable to resonant state (quenching)
7	$2Ar_m^* \rightarrow e_{fast} + Ar + Ar^+$	—	$k_p = 1 \times 10^{13}\ m^3\ s^{-1}$ [35]	Penning ionization
8	$2Ar_r^* \rightarrow e_{fast} + Ar + Ar^+$	—	$k_p = 1 \times 10^{13}\ m^3\ s^{-1}$ [35]	Penning ionization
9	$Ar_m^* + Ar_r^* \rightarrow e_{fast} + Ar + Ar^+$	—	$k_p = 1 \times 10^{13}\ m^3\ s^{-1}$ [35]	Penning ionization
10	$Ar_r^* \rightarrow Ar + hv$	—	$A_R = 3 \times 10^6\ s^{-1}$	Resonance radiation with adjustment for self-absorption ($\gamma = 106.4$ nm)
11	$e + Ar_m^* \rightarrow e_{fast}$	—	$K_p = 4 \times 10^{-16}\ s^{-1}$	Superelastic collision

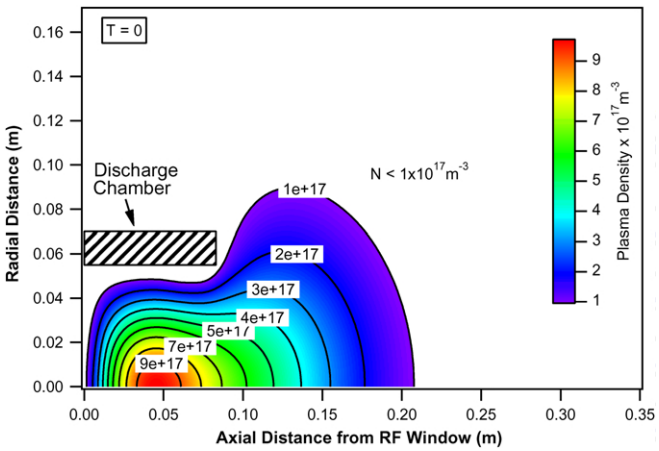

Figure 2. Spatial distribution of electron density at the end of the active phase.

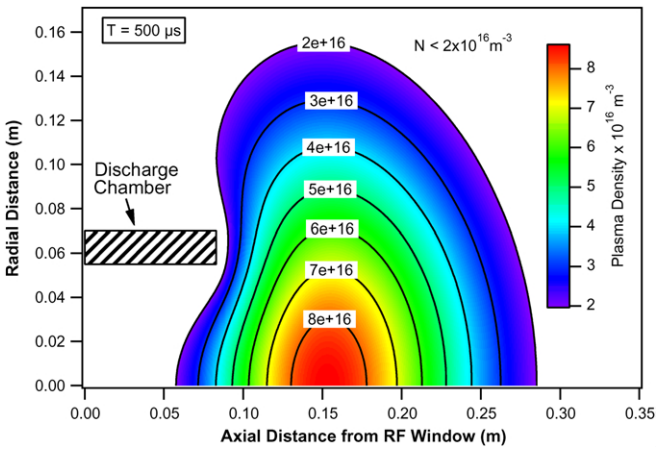

Figure 3. Spatial distribution of electron density at $t = 500\,\mu$s in the afterglow.

far from the rf window and due to ambipolar diffusion, extends somewhat into the large ballast volume (see figure 2). Again, as one would expect, electrons are generated in the small discharge chamber and act as a source for the ballast chamber. In the afterglow, the peak electron density moves outside the discharge chamber into the ballast volume (see figure 3). The overall density has decreased in the afterglow, but the peak value is now located in the ballast volume. In this case, the ballast volume acts as a source of electrons for the discharge chamber. Thus, during the active phase the ballast volume has only a small effect on the behavior in the discharge volume, but during the afterglow phase the ballast volume is a significant perturbation on the discharge chamber.

Table 2. Spatially averaged plasma parameters for the discharge chamber 'open' and 'closed' geometry.

End active phase	N_e (m^{-3})	N_m (m^{-3})	T_e (eV)
Open	3.2×10^{17}	2.6×10^{17}	2.4
Closed	4.5×10^{17}	2.8×10^{17}	2.56

In order to demonstrate this behavior more clearly, special simulations were performed for the device as shown in figure 1 (henceforth referred to as 'open' geometry) and for the case when the opening of the discharge chamber is closed by an additional wall (henceforth referred to as 'closed' geometry), for the same excitation conditions. Table 2 shows the Spatially averaged parameters of the plasma in the small chamber at the end of the active phase for the two cases. As seen in the table, the values calculated for the open and closed discharge chamber, during the active phase, are reasonably close in value. Therefore, during the active phase the presence of the ballast chamber has only a small effect on the parameters of the plasma in the discharge chamber. This can be explained on the basis of the simple balance of quasistationary plasma during the active phase, that is, the balance of creation and diffusion decay of charged particles to the walls ($\nu_i \tau_a = 1$). Since all of the applied power goes into the small chamber, even a much slower diffusion loss of plasma in the ballast chamber cannot compensate for the low rate of its production (the only charged-particle source is the 'outflow' from the discharge chamber). Under conditions of equal applied power, the differences between diffusion lengths (we use 'O' and 'C' to designate open and closed geometry) Λ_O and Λ_C can be approximated by

$$\frac{1}{\Lambda_C^2} = \frac{2.4^2}{R^2} + \frac{\pi^2}{H^2} \qquad \text{and} \qquad \frac{1}{\Lambda_O^2} = \frac{2.4^2}{R^2} + \frac{\pi^2}{4H^2}, \quad (1)$$

which leads to $\Lambda_C < \Lambda_O$ and their effective diffusion times $\tau_C < \tau_O$. The somewhat higher values for electron density and temperature seen for the closed geometry in table 2 are due to this decreased diffusion time, which for equal power

results in an increased T_e and ionization rate (as the diffusion rate increases, the ionization rate must increase to balance the loss).

Now consider the afterglow phase, where, in contrast to the active phase, there is a significant difference in the plasma characteristics with or without the ballast volume. As expected, in the simplest case (closed), when there is only a small chamber (i.e. no ballast volume) evolution of the plasma density has the well-known behavior in the form

$$\frac{dN_e}{dt} = -\frac{N_e}{\tau_a} \qquad \text{or} \qquad N_e(t) = N_e(0)\exp\left(-\frac{t}{\tau_a}\right) \tag{2}$$

with the characteristic time for ambipolar diffusion to the wall (see, for example, [1])

$$\tau_a = \frac{\Lambda_C^2}{D_a} \tag{3}$$

with $D_a = D_i(1 + T_e/T_i)$. This case is well-studied and lies within the framework of the global model. A comparision between results from the simulation data and calculations using equation (2), with temperatures taken from the simulations, agree very well. For this simple, closed geometry case, calculations show the density and temperature of the plasma electrons fall monotonically, while maintaining a spatial distribution close to the fundamental diffusion mode.

For the case of discharge chamber with additional ballast volume, results proved to be unexpectedly different from the previous, standard situation. In this case, the spatial distribution of the afterglow plasma changes significantly from what might be expected. Specifically, the maximum in the plasma density moves from the discharge chamber to the diffusion chamber, as shown in figures 2 and 3. Figures 4 and 5 show the temporal change of average plasma parameters in the discharge chamber for both the closed regime (dashed lines) and open regime (solid lines).

It can be seen that the fall in T_e for the closed geometry is faster than for the open case. As previously discussed, this can be attributed to the smaller characteristic diffusion length for the closed case and a faster diffusion cooling rate. With the higher T_e seen for the open geometry, one would expect a higher ambipolar diffusion rate and therefore a faster decay of N_e in the small chamber. However, as seen in figure 5, the decay of N_e in the discharge chamber is slower for the open geometry than the closed geometry. This indicates that the discharge chamber has recieved an additional flux of charged particles from the ballast volume, which compensates for their decay at the walls.

Figure 6 shows the temporal (in the afterglow) and axial behavior of N_e in the system for both the open and the closed geometries. The dashed lines correspond to the closed geometry, and solid lines correspond to the open case. As can be seen from figure 6, the density of plasma in the ballast volume, which is much less than the density in the discharge chamber during the active phase, maintains this behavior only at the beginning of afterglow. Because of a substantial difference in the size of volumes, decay of the plasma in the ballast is much slower than in the discharge volume. Because of this, the electron density in the discharge chamber will be smaller than the density in the ballast volume for only the first 30 μs into the afterglow. The plasma density gradient in the

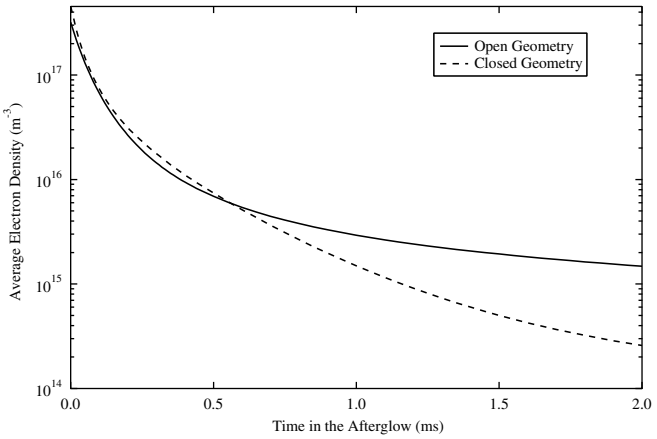

Figure 4. Temporal behavior of averaged N_e in the discharge chamber.

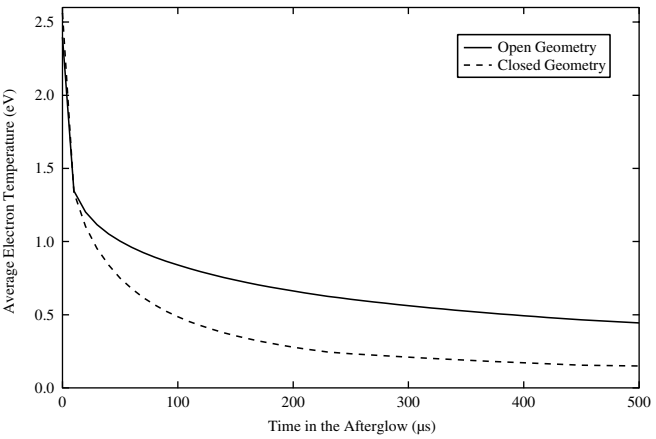

Figure 5. Temporal behavior of averaged T_e in the discharge chamber.

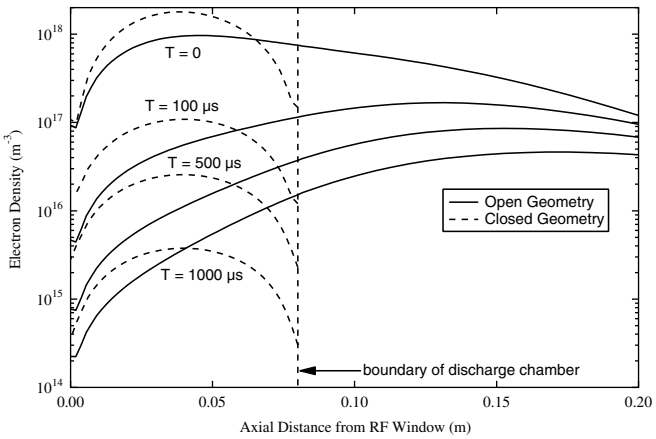

Figure 6. Axial and temporal behavior of N_e for the closed and open geometries. Times are relative to rf cut-off.

axial direction changes sign or diffuses in the opposite direction from that seen in the active phase (see figure 7). The upshot is that roughly speaking, during the active phase plasma flows out of the discharge chamber, while in the afterglow it flows back. Thus, the ballast volume plays the role of a thermostat.

Lastly, figure 7 shows the temporal behavior of the total ambipolar flux crossing the imaginary surface between the discharge and the ballast chambers. Here, a positive flux indicates an outflow from the small to the large chamber and

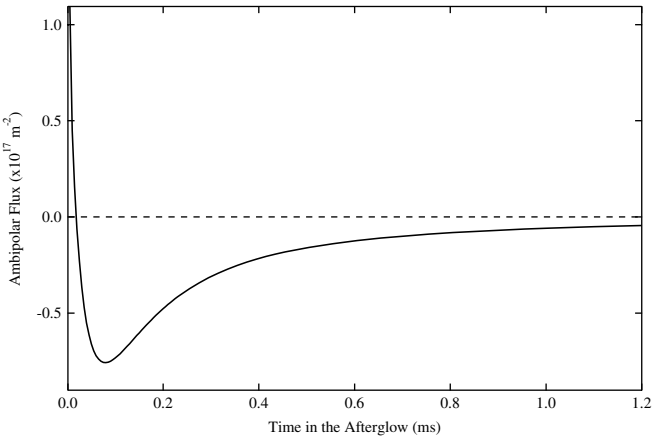

Figure 7. Temporal behavior of the ambipolar flux incident on the imaginary boundary between the two chambers.

time is referenced to shut-off of the rf power (afterglow). As is clear from the figure, the flux changes sign during the afterglow. This indicates that the ambipolar electric field also changes sign. This curious phenomenon of the change in the direction of flux and ambipolar field should be taken into account in estimating the properties for pulsed plasmas in these types of reactors. In particular, estimates of the plasma parameters in the small chamber, during the afterglow phase, based on the global model may lead to not only quantitative but even qualitative errors. Note that in multi-component gas mixtures, the effects may have additional manifestations and consequences. For example, in the presence of negative ions trapped by the ambipolar field, which is created by more mobile electrons, it is possible to expect a variety of scenarios for the evolution of the plasma pulse. A more detailed investigation is required for this interesting case of a multi-component plasma, containing negative ions.

5. Conclusions

Cylindrically symmetric 2D, time dependent simulations of a pulsed (100% modulated) ICP in argon have been performed for the case of a small discharge chamber connected to a much larger ballast volume. During the active phase of the discharge, plasma is formed in the small chamber and diffuses to the large ballast volume. Due to the localized plasma production at the rf window of the small chamber, the plasma density in the ballast volume is relatively low. As a result, the presence of the ballast volume is not a significant perturbation on the discharge chamber plasma properties during the active phase. This occurs despite a much slower rate of diffusion to the walls in the large chamber.

The situation is quite different during the afterglow phase, primarily as a result of the large differences in diffusion times between the two chambers. Without an external source of ionization, the much shorter diffusion time in the discharge chamber causes the plasma density to drop rapidly below that in the ballast volume. This is now opposite to the situation that exists during the active phase. During the afterglow, plasma from the ballast volume is a large perturbation on the plasma characteristics in the discharge chamber and acts as a long-lived source of charged particles for the smaller volume. Since this subject has not been well covered in the literature, it would be especially interesting to explore these phenomena in complex mixtures, specifically, in electronegative gases.

Acknowledgments

This work was supported in part by the Air Force Office of Scientific Research. In addition, authors EAB, AAK and KYuS received support from the US Civilian Research and Development Foundation (CRDF) and author VID was supported with a grant from the Defense Experimental Program to Stimulate Competitive Research (DEPSCoR).

References

[1] Lieberman M A and Lichtenberg A J 2005 *Principles of Plasma Discharges and Material Processing* (New York: Wiley)
[2] Kogelschatz U 2002 *Plasma Sources Sci. Technol.* **11** A1
[3] http://www.kinema.com/
[4] http://www.cfdrc.com/
[5] http://uigelz.ece.iastate.edu/
[6] Bukowski J D, Graves D B and Vitello P. 1996 *J. Appl. Phys.* **80** 2614
[7] Lymberopoulos D P, Kolobov V I and Economou D J 1998 *J. Vac. Sci. Technol.* A **16** 564
[8] Betle S, Brockhaus A and Endemann J 2000 *Plasma Source Sci. Technol.* **9** 57
[9] Kiehlbauch M W and Graves D B 2002 *J. Appl. Phys.* **91** 3539
[10] Robson R E, White R D and Petrovic Z Lj 2005 *Rev. Mod. Phys.* **77** 1303
[11] Kim H C, Iza F, Yang S S, Radmilovic-Radjenovic M and Lee J K 2005 *J. Phys. D: Appl. Phys.* **38** R283
[12] Subramonium P and Kushner M J 2002 *J. Vac. Sci. Technol.* A **20** 313
[13] Phelps A V 1990 *J. Res. Natl Inst. Stand. Technol.* **95** 407
[14] Lee C, Graves D B, Lieberman and Hess D W 1994 *J. Electrochem. Soc.* **141** 1546
[15] Lee C and Lieberman M A 1995 *Plasma Source Sci. Technol.* **5** 145
[16] Lieberman M A and Ashida S 1996 *Plasma Source Sci. Technol.* **5** 145
[17] Kimura T and Ohe K 2001 *J. Appl. Phys.* **89** 4240
[18] Demidov V I, DeJoseph C A Jr and Kudryavtsev A A 2004 *Phys. Plasmas* **11** 5350
[19] Demidov V I, DeJoseph C A Jr and Kudryavtsev A A 2004 *Plasma Sources Sci. Technol.* **13** 600
[20] Demidov V I, DeJoseph C A Jr and Kudryavtsev A A 2005 *Phys. Rev. Lett.* **95** 215002
[21] Godyak V A, Piejak R B and Alexandrovich B M 2002 *Plasma Sources Sci.Technol.* **11** 525
[22] Tadokoro M, Hirata H, Nakano N, Petrovic Z and Makabe T 1998 *Phys. Rev.* E **58** 7823
[23] Okigawa A, Makabe T, Shibagaki T, Nakano N, Petrovic Z, Kogawa T and Itoh A 1996 *Japan. J. Appl. Phys.* **35** 1890
[24] Makabe T and Petrović Z 2002 *Appl. Surf. Sci.* **192** 88
[25] Bogdanov E A, Kudryavtsev A A and Arslanbekov R R 2006 *Contrib. Plasma Phys.* **46** 807
[26] Bogdanov E A, Kudryavtsev A A, Arslanbekov R R and Kolobov V I 2004 *J. Phys. D: Appl. Phys.* **37** 2987
[27] Pichford L C, Kang J, Punset C and Boeuf J P 2002 *J. Appl. Phys.* **92** 6990
[28] 1999–2006 *CFD-PLASMA: User's Manual* (Huntsville, TX: CFD)
[29] Bogdanov E A, Kudryavtsev A A, Arslanbekov R R and Kolobov V I 2004 *J. Phys. D: Appl. Phys.* **37** 2987
[30] Arslanbekov R R, Kolobov V I, Bogdanov E A and Kudryavtsev A A 2004 *Appl. Phys. Lett.* **85** 3396
[31] Bogdanov E A, Kudryavtsev A A, Tsendin L D, Arslanbekov R R and Kolobov V I 2004 *Tech. Phys.* **49** 849

AQ2

AQ3

[32] Bogdanov E A, Kudryavtsev A A, Tsendin L D, Arslanbekov R R, Kolobov V I and Kudryavtsev V V 2003 *Tech. Phys.* **48** 1151
[33] Phelps A V 1985 *JILA Report No* 28 jila.colorado.edu/collision_data/electronneutral
[34] Hayashi M Ar cross section set jila.colorado.edu/collision_data/hayashi.txt
[35] Bogaerz A and Gijbels R 1995 *Phys. Rev.* A **52** 3743
[36] Vriens L, Keijser R and Ligther F 1978 *J. Appl. Phys.* **49** 3807